

# CFD SIMULATION OF VORTEX RING FORMATION FOR LOW SPEED IMPULSIVE PROPULSION

XIAOSONG ZHANG, DECHENG WAN\*

State Key Laboratory of Ocean Engineering, School of Naval Architecture, Ocean and Civil Engineering, Shanghai Jiao Tong University, Collaborative Innovation Center for Advanced Ship and Deep-Sea Exploration, Shanghai 200240

\*Corresponding Author: dcwan@sjtu.edu.cn

**Keywords:** Impulsive propulsion; Vortex ring formation; OpenFOAM; Piston-nozzle apparatus

Impulsive propulsion is a kind of bionic propulsion, whose concept comes from the squid. Squid generates an impulsive jet for thrust through its body muscle contraction. During the process of impulsive propulsion, large-scale vortex ring is generated in the near-wake, which plays an important role in the efficiency promotion. In recent years, some small underwater vehicles are equipped with Vortex Ring Thruster (VRT). In this paper, open source platform OpenFOAM is applied to numerically investigate the vortex ring behaviour during the propulsion process. A piston-nozzle apparatus is applied to simulate thruster. Mesh sensitivity study is firstly conducted. Vortex rings behaviour in calm water under different stroke ratios are simulated. The calculated vortex ring formation and pinch-off phenomenon are in good agreement with experimental results. In addition, vortex ring formation is investigated in the presence of background flow. The vortex ring is found smaller and the “pinch-off” phenomenon is delayed by the background flow. Besides, cyclic pulse simulation is carried out. The simulation indicates that there exists reverse vorticity during cyclic pulse process, which can reduce the energy of vortex rings.

## Introduction

As a result of natural selection, fast moving marine animals choose impulsive modes to swim. This type of impulsive propulsion like squid has high efficiency. For ship and marine vehicle, propeller is the most commonly used propulsion device. Because of the spin of blades in water, the kinetic energy built up in water is contributed not only from the speedup water velocity in line with the thrust direction but also from the swirl velocity of water associated to the spin of the blades. Water kinetic energy due to the swirl of water doesn't contribute to the generation of thrust and therefore it is an energy waste. However, impulsive propulsion can avoid the swirl energy loss. Thus, it is very meaningful to develop impulsive propulsion.

Vortex rings are a typical phenomenon in impulsive. A great amount of experimental works have been carried out to study vortex rings through the starting flows generated from a piston-nozzle apparatus. Gharib et al.<sup>[1]</sup> proposed a universal time scale for vortex ring formation, which showed that the large-scale vortex followed by a trailing jet only occurred when stroke ratio is larger than 4. On the other hand, when stroke ratio is smaller than 4, the flow field consists of only a single vortex ring. Rosenfeld et al.<sup>[2]</sup> carried out CFD simulation of the vortex formation in calm water, the influence of three different kinds of geometric shapes were discussed. Krueger et al.<sup>[3-4]</sup> analysed the influence of vortex ring on thrust of thruster. The contribution of vortex ring was attributed to the change of fluid pressure, which was named “over-pressure”. Furthermore, Krueger et al.<sup>[5]</sup> studied experimentally the vortex ring pinch-off process in the presence of a simultaneously initiated uniform background co-flow and found that the formation number was reduced by background flow. Jiang et al.<sup>[6]</sup> carried out numerical simulation to study the vortex formation in the presence of a fully developed background flow and described the interaction between vortex ring and background flow vorticity.

In this paper, CFD solver *pimpleDyMFoam* in OpenFOAM was used to solve the impulse problem and the vortex ring formation process in background flow conditions. Cyclic pulse simulations were also carried out to investigate the interaction between vortex rings.

## Numerical method

In present work, the three dimensional time-dependent incompressible Navier-Stokes equations are employed for simulating the flow. The governing equations can be written as follows:

$$\nabla u_i = 0 \quad (1)$$

$$\frac{\partial u_i}{\partial t} + (u_i \cdot \nabla) u_i = -\nabla p + \nu \nabla^2 u_i \quad (2)$$

where  $u_i$  is velocity in three direction ( $i = x, y, z$ ),  $\nabla$  is divergence operator,  $\nabla^2$  is Laplace operator,  $\nu$  is the fluid kinematic viscosity.

In order to simulate piston-nozzle jet, moving mesh technology is used to control the piston motion. The mesh motion is obtained by solving a mesh motion equation, where boundary motion acts as a boundary condition and determines the position of mesh points. The motion is characterized by the spacing between nodes, which changes by stretching and squeezing.

In this study, the velocity of mesh motion  $u_g$  is obtained by solving a Laplace equation as follows:

$$\nabla \cdot (\gamma \nabla \mathbf{u}_g) = 0 \quad (3)$$

By this velocity, the mesh move forward to a new position:

$$X_{new} = X_{old} + \mathbf{u}_g \Delta t \quad (4)$$

The coefficient  $\gamma$  in Eqn. (3) is the diffusion coefficient, which is used to control the mesh spacing and quality. The definition of  $\gamma$  is:

$$\gamma(r) = \frac{1}{r^m} \quad (5)$$

where  $r$  is the radius from the moving boundary,  $m$  is an integer. In this study, for x direction,  $m$  is set to 1 to obtain an appropriate mesh motion, for y direction and z direction,  $m$  is set to a very large number so that the mesh motion in these two direction are restrained.

### Geometry and computational condition

A piston-nozzle apparatus was applied to simulate thruster. The computational domain consisted of nozzle and outer flow domain is shown in Figure 1. Dimension of the piston is exactly the same with previous experiments of Gharib et al.<sup>[1]</sup>. The inner diameter ( $D$ ) of nozzle is 2.54cm, sharp-wedged exit nozzle shape with a tip angle of  $20^\circ$  is adopted. The total length of the piston is 40cm. The outer flow domain span  $10D$  in the streamwise direction and  $2.5D$  in the radial direction.

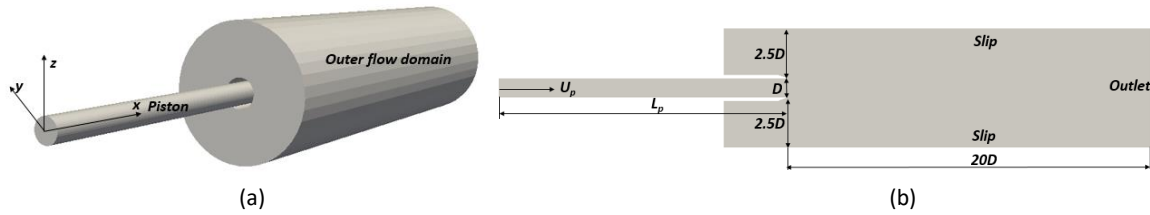


Figure 1 The computational domain. (a) Three-dimensional view of the numerical domain. (b) Domain dimension and boundary condition.



Figure 2 Details of mesh arrangement. (a) Overall mesh arrangement. (b) Local mesh around the nozzle exit

Figure2 shows the detailed mesh arrangement. Mesh in the nozzle is uniform in three directions and is gradient distribution in the radial direction for outer flow domain. According to previous literature, it is essential to accurately calculate the friction which plays an important role in the formation of vortex. Friction test has been performed by simulating pipe flow cases using the nozzle geometry with different mesh arrangements. The friction calculated with  $80 \times 50 \times 40$  meshes in the axial, radial and circumferential directions is accurate enough. This mesh arrangement is adopted for nozzle mesh. For the outer flow domain, pressure of specific point was applied for mesh sensitivity test. It avoids the problem in the previous numerical researches' mesh sensitivity test<sup>[2][6]</sup> that total circulation cannot reflect the particulars. The specific point is on the central axis of the nozzle and  $2D$  distance away from the nozzle exit. Test results are shown as Figure 3.

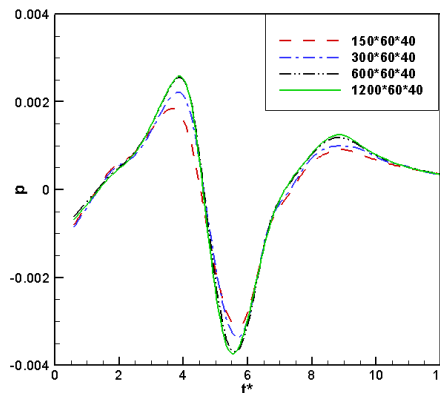


Figure 3 Mesh sensitivity test in axial and radial direction.

On the basis of results of mesh sensitivity test,  $600 \times 60 \times 40$  meshes in the axial, radial and circumferential directions is adopted in the outer flow domain.

## Numerical results and analysis

In order to better represent the results of the calculation, two non-dimensional times are defined as:

$$T^* = L_m/D = U_p T/D \quad (6)$$

$$t^* = L/D = U_p t/D \quad (7)$$

where  $L_m$  is piston stroke,  $L$  is the distance of piston motion,  $D$  is the inner diameter of nozzle.  $U_p$  is piston velocity.

The comparison between CFD results and experimental results in calm water condition under different stroke ratios ( $T^* = 2, 3.8, 14.5$ ) is shown in Figure 4.

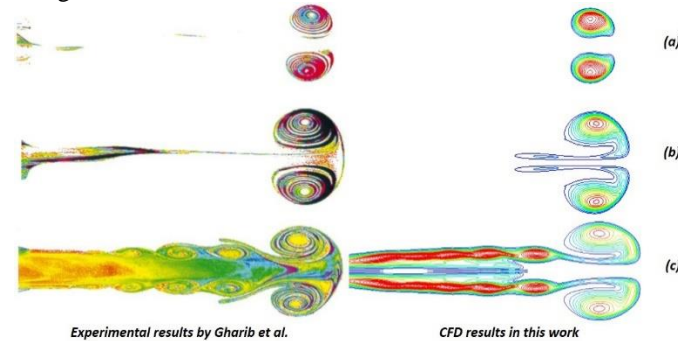


**Figure.4 Comparison of vortex ring between CFD results in this work and experimental results by Gharib et al. (a)  $T^*=2$ ; (b)  $T^*=3.8$ ; (c)  $T^*=14.5$ .**

It is obvious that the CFD results are in good agreement with the experimental results regarding to the vortex ring formation. For the case  $T^* < 4$  (a), the leading vortex is small and there is no trailing vorticity behind the vortex ring; For the case  $T^* \approx 4$  (b), it appears that the leading vortex ring is nearly saturated; For the case  $T^* > 4$  (c), there is an obvious trailing vorticity behind the leading vortex ring and there are some small vortex in the trailing flow. It is universally accepted that the “Formation number” is nearly equal to 4 for single pulse vortex ring.

According to above phenomena, trailing vorticity flow appears when  $T^* > 4$ . Under this condition, another important phenomenon “pinch-off” will occur in the propagation process. The formation and propagation of the vortex ring for  $T^* = 6$  is shown in Figure 5.

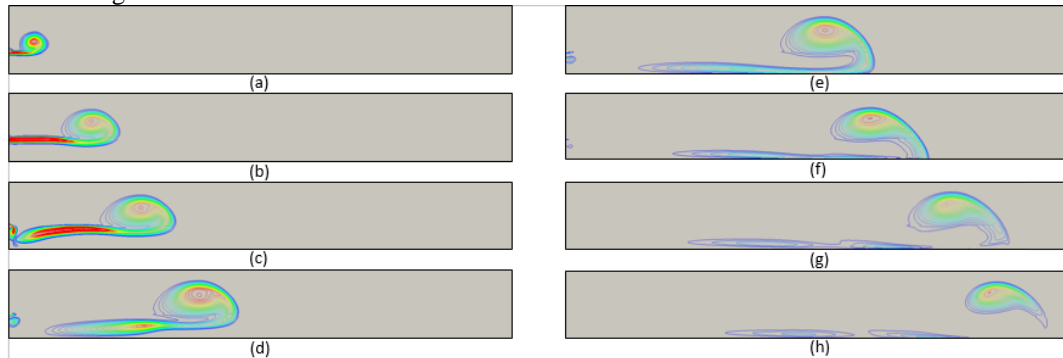


**Figure.5 The formation and propagation of the vortex ring for single pulse  $T^*=6$  in calm water. The formation times are  $t^*=1.5$  (a),  $t^*=4.5$  (b),  $t^*=6.6$  (c),  $t^*=9$  (d),  $t^*=12$  (e),  $t^*=15.6$  (f),  $t^*=19.5$  (g),  $t^*=21.6$  (h).**

In the case of small piston ratio, all the vorticity generated at the nozzle during the ejection is essentially entrained into the downstream propagating vortex ring. However, the situation is different for the case of large piston ratio ( $T^* > 4$ ) as shown in Figure 5. At first, due to the action of shear layer, a large-scale vortex ring is formed at the nozzle exit. With the push of the piston, a striped wake vorticity arises behind the vortex ring. When the piston stop at time instant (c), striped wake vorticity breaks down from the nozzle. Then the leading vortex moves forward with an obvious trailing vorticity behind it. Because the energy of vortex is saturated, the trailing vorticity cannot get into the vortex, and the trailing vorticity becomes longer and longer. The large-scale leading vortex contain larger energy and move faster, then the “pinch-off” phenomenon occurs (f). The vortex ring disconnects itself from the bulk of the flow, leaving behind a noticeable tail of vorticity flow region.

For actual propulsion, the ambient fluid should not be calm water condition. Thus, it is necessary to place this apparatus into an environment with ambient flow to investigate vortex ring formation in the presence of background flow. As for CFD measure, the boundary conditions were changed as the Figure 6 to simulate the ambient flow.

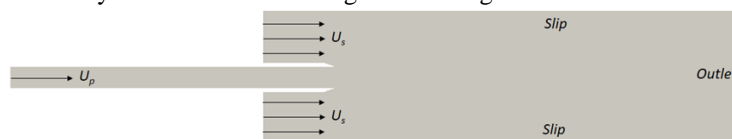


**Figure 6 Boundary conditions of case with ambient flow.**

where  $U_s$  is the ambient velocity. For the thruster,  $U_s$  is equivalent to advance velocity. The evolution of the vorticity field for the case of  $U_s = 0.5U_p$  is as shown in Figure 7.

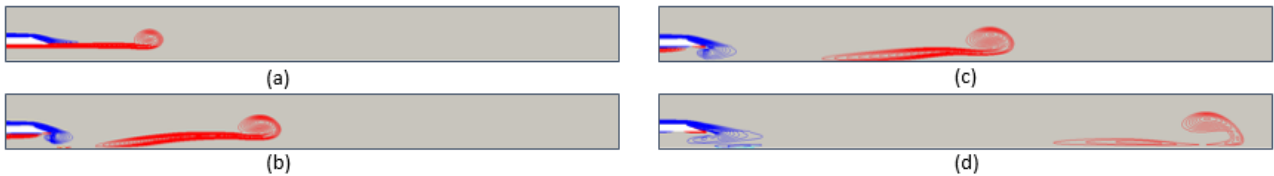


**Figure.7 The formation and propagation of the vortex ring for single pulse  $T^*=6$  with background flow  $U_s = 0.5U_p$ . The formation times are  $t^*=4.5$  (a),  $t^*=9$  (b),  $t^*=12$  (c),  $t^*=20.4$  (d)**

The influence of background flow field on vortex ring can be seen from Figure 7. Vorticity is coloured by rotation directions of vortex. At first, the vortex ring is smaller and trailing vorticity is longer obviously in contrast with the calm water condition at the same time. Besides, there is obvious reverse vorticity around the nozzle exit, which can consume the energy of vortex during the formation process. In addition, the “pinch-off” phenomenon is delayed by the background flow. It occurs at the time  $t^*=20.4$  as Figure 7 (d) shows, while it occurs at the time  $t^*=15.6$  in calm water condition as Figure 5 (f) shows.

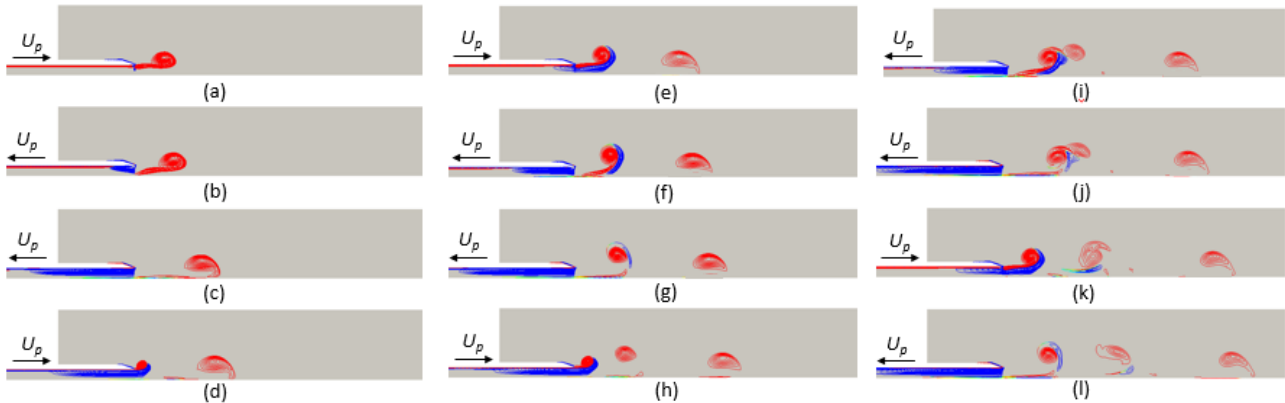


**Figure.8 The formation and propagation of the vortex ring for cyclic pulse  $T^*=3.9$  in calm water. The formation times are  $t^*=1T^*$ (a),  $t^*=1.2T^*$ (b),  $t^*=2T^*$ (c),  $t^*=2.3T^*$ (d),  $t^*=3T^*$ (e),  $t^*=3.5T^*$ (f),  $t^*=4T^*$ (g),  $t^*=4.5T^*$ (h),  $t^*=5.5T^*$ (i),  $t^*=6T^*$ (j),  $t^*=7T^*$ (k),  $t^*=8T^*$ (l)**

For vortex ring thruster, the thrust produced by the piston in the apparatus for reciprocating motion to breathe and remove the liquid. Since vortex ring plays an important role in the thrust production, it is significant to study the formation and propagation of the vortex ring for cyclic pulse. The detailed process is in Figure 8.  $T^*=3.9$  was selected because it is a critical saturation state for vortex ring as mentioned above. Vorticity is coloured by rotation directions of vortex. Firstly, a large-scale vortex ring generated by the first push just like the single pulse. Then the piston begin to shrink, when water is sucked into the nozzle, it will generate reverse vorticity through the nozzle exit. A long vorticity strip is formed when the piston shrinks to the limit position. Then the second pulse begins, fluid in the boundary layer is pushed pass the exit and generate a vortex ring (red in the Figure), while the vorticity strip is pushed out at the same time. During the propagation, the vortex strip is tightly attached to the vortex ring. Because of the difference of rotation direction, interaction consumes the energy of vortex ring, which contributes to volume reduction and speed reduction. Consequently, the reverse vorticity strip is exhausted, and the vortex ring becomes an isolated small vortex ring. Because the speed of the second vortex ring is very slow, it will be overtaken by the third vortex ring surrounded with vorticity strip at time instant (i), the vorticity strip is consumed by both the third vortex ring and the second vortex ring, and these two vortex rings are synthesized as one vortex ring as (k) shows. Every two pulses after will repeat the previous cycle (d-k).

It has been proposed previously that vortex ring can improve the efficiency of propulsion by the entrained fluid<sup>[3][4]</sup>. In the present work, it is also noted that the reverse vorticity in cyclic pulse condition that can reduce the energy of vortex ring as mentioned above, which results in reduction of fluid entrainment.

## References

- [1] MORTEZA GHARIB, EDMOND RAMBOD, KARIM SHARIFF. A universal time scale for vortex ring formation[J]. Journal of Fluid Mechanics. 1998, 360: 121-140.
- [2] MOSHE ROSENFELD, EDMOND RAMBOD, MORTEZA GHARIB. Circulation and formation number of laminar vortex rings[J]. Journal of Fluid Mechanics. 1998, 376: 297-318.
- [3] PAUL S. KRUEGER. The significance of vortex ring formation and nozzle exit over-pressure to pulsatile jet propulsion[D]. California Institute of Technology Pasadena, California, 2001.
- [4] PAUL S. KRUEGER, M. GHARIB. The significance of vortex ring formation to the impulse and thrust of a starting jet[J]. Physics of Fluids. 2003, 15(5): 1271-1281.
- [5] PAUL S. KRUEGER, JOHN O. DABIRI, M. GHARIB. Vortex ring pinch-off in the presence of simultaneously initiated uniform background co-flow[J]. Physics of Fluids. 2003, 15: L49-L52.
- [6] HOU SHOU JIANG, MARK A. GROSENBAUGH. Numerical simulation of vortex ring formation in the presence of background flow with implications for squid propulsion. Theoretical and Computational Fluid Dynamics. 2006, 20(2): 103-123.